

Condensation and Intermittency in an Open Boundary Aggregation-Fragmentation Model

Himani Sachdeva,¹ Mustansir Barma,¹ and Madan Rao^{2,3}

¹*Department of Theoretical Physics, Tata Institute of Fundamental Research,
Homi Bhabha Road, Mumbai-400005, India*

²*Raman Research Institute, C.V. Raman Avenue, Bangalore 560080, India*

³*National Centre for Biological Sciences (TIFR), Bellary Road, Bangalore 560065, India*

We study real space condensation in aggregation-fragmentation models where the total mass is not conserved, as in phenomena like cloud formation and intracellular trafficking. We study the scaling properties of the system with influx and outflux of mass at the boundaries using numerical simulations, supplemented by analytical results in the absence of fragmentation. The system is found to undergo a phase transition to an unusual condensate phase, characterized by strong intermittency and giant fluctuations of the total mass. A related phase transition also occurs for biased movement of large masses, but with some crucial differences which we highlight.

PACS numbers: 05.40.-a, 05.60.Cd, 64.60.-i

Condensation transitions constitute an important class of non-equilibrium phase transitions, and occur generically in many mass transport models [1] such as the zero range process and its variants [2], and the aggregation-chipping model [3]. These systems are characterized by a fixed total mass (number of particles) and stochastic rules for exchange of mass between sites. When the total mass of the system exceeds a critical value, condensation sets in, with a finite fraction of the total mass forming a macroscopic cluster that occupies a single site. The phenomenon is akin to Bose condensation, but in real space.

Does the condensation transition survive in a system when the total mass is not conserved, but can undergo large fluctuations due to the exit of clusters of all sizes? This question is important in a number of physical situations, ranging from formation of clouds and aerosols, to intracellular trafficking and organelle formation in living cells [4–6]. We address this within a simple but generic 1D model with aggregation and fragmentation (chipping) of masses in the bulk, and influx and outflux of masses at the boundaries. Our main finding is that the open system *does* undergo a condensation transition upon increasing the influx or decreasing the chipping rate. However, the nature of the condensate is very different from that in the closed model [3], in that the mass in the condensate shows giant number fluctuations and has a broad distribution, in contrast to the sharply peaked distribution in the closed system [3, 7]. The condensate, however has a well-defined, finite mean mass for a fixed system size and is thus quite different from the indefinitely growing aggre-

gates in open models which allow only single particles to exit at the boundaries [6, 8].

The intermittent and fluctuating nature of the condensate gives rise to novel signatures: the total mass M itself shows giant fluctuations and has a distribution characterized by a prominent non-Gaussian condensate tail whose width scales with system size. Further, the exit of the condensate from the boundaries and the accompanying sharp drops in M give rise to interesting ‘charge and fire’ behaviour of M : the time series $M(t)$ departs strongly from self-similarity and shows quantitative features of intermittency, which we characterize in terms of appropriately defined structure functions, as in turbulence phenomena. Turbulence, in the sense of multi-scaling of n -point mass-mass correlation functions has been studied earlier in aggregation models [9], but our characterization of turbulence-like behaviour is quite different, being associated with *temporal* fluctuations of *total* mass. Our results are based on both analytical and numerical work. In the limit of zero chipping, we analytically calculate the moments of total mass in steady state, and also the dynamical structure functions, whereas for non-zero chipping, we perform numerical Monte Carlo simulations.

Recently, it has been demonstrated that giant number fluctuations are related to anomalous, non-Porod behaviour of spatial correlation functions in a wide class of systems [10]. Our work points to a connection between giant number fluctuations and anomalous dynamical behaviour, namely temporal intermittency, which is related to higher order correlation functions *in time* [12]. It also raises the

interesting general question of whether temporal intermittency is present in other systems with giant number fluctuations and suggests that dynamical structure functions, as used in the paper, provide a useful probe of intermittency in these systems also.

We work with a general lattice model incorporating diffusion, aggregation, fragmentation, influx and outflux, which goes beyond earlier studies of aggregation with input [13–15], and aggregation and fragmentation in a closed system [3, 16]. Starting with an empty lattice of L sites at $t = 0$, a site i is chosen at random, and one of the following moves occurs:

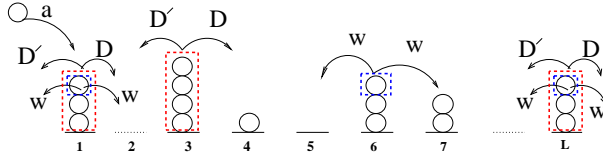


FIG. 1. Model: Influx of unit masses at site 1. Forward and backward stack movement at rates D and D' respectively. Forward and backward chipping at equal rates w . Outflux of full stack or unit mass (via chipping) from site L (and 1).

- i. Influx: A single particle of unit mass is injected at rate a at the first site ($i = 1$).
- ii. Diffusion and aggregation: With rate D (or D'), the full stack on site i (i.e. all particles on the site collectively) hops to site $i + 1$ (or $i - 1$) and adds to the mass already there.
- iii. Chipping of unit mass: With rate $2w$, a unit mass breaks off from the mass at i and hops to site $i - 1$ or $i + 1$ with equal probability, adding to the mass already there.
- iv. Outflux of mass from boundaries: With rate D (or D'), the entire mass at site L (or site 1) exits the system; with rate w , a unit mass breaks off from site L (or site 1) and exits.

We find that the results depend strongly on two factors: one, whether motion of particles is biased or not and two, whether or not exit of masses is allowed from the boundary where influx occurs. In this paper, we only consider the effect of bias [11]. We find that the occurrence of the phase transition is robust with respect to bias in the movement of stacks, but not chipping. As in the closed periodic case, if the

forward and backward chipping rates are unequal, an aggregate is not expected to form [17]. Thus, chipping is taken to be unbiased in both the cases we study in this paper:

(A) *Unbiased Stack Hopping*: $D = D'$; exit allowed from sites 1 and L .

(B) *Biased Stack Hopping*: $D' = 0$; exit allowed from site L

Influx and chipping occur at rates a and $2w$ respectively in both the above.

(A) Unbiased Stack Hopping ($D' = D$): We discuss both the phases and the critical point below:

Normal (large w) phase: In this phase, a typical configuration does not show very large fluctuations about the average mass profile. The total mass M too has normal fluctuations i.e. the rms fluctuations $\Delta M \equiv \sqrt{\langle M^2 \rangle - \langle M \rangle^2} \propto \sqrt{L}$, with the distribution for the rescaled mass variable $(M - \langle M \rangle)/\Delta M$, approaching a Gaussian at large L . The mass distribution $P(m, j, L)$ at a given site j is found to depend on j and L only through the rescaled position variable $x = j/L$ [18], implying that for a given x , all moments of mass are independent of L to leading order.

Condensate (small w) phase: A typical configuration deviates strongly from the average profile, with the largest (local) fluctuations scaling as system size L . On monitoring the largest mass m_1 in the system, we find that its average value $\langle m_1 \rangle$ is proportional to L [18], implying that the system contains a macroscopic condensate. The presence of the condensate has a strong effect on all steady state properties of the system such as the total mass M , mass at a site, etc. The probability distributions of all these quantities have an exponential tail with a characteristic mass M_0 where $M_0 \propto L$ for a given w and a . We refer to this exponential tail as the ‘condensate’ tail and describe below, how it appears in various steady state distributions:

- i. The steady state distribution $P(M)$ of total mass of M in the system behaves as $P(M) \sim \frac{1}{M_0} \exp\left(-\frac{M}{M_0}\right)$ at large M [fig. 2]. Consequently, the rms fluctuation ΔM of total mass shows non-Gaussian behaviour, scaling as L rather than \sqrt{L} . We have analytically calculated various moments of the total mass in the limit $w = 0$ [18]. We find that $\Delta M/L \simeq 0.46(a/D)$, in the limit of large L , which agrees well with numerics.
- ii. The distribution $P(m_1)$ of the largest mass m_1

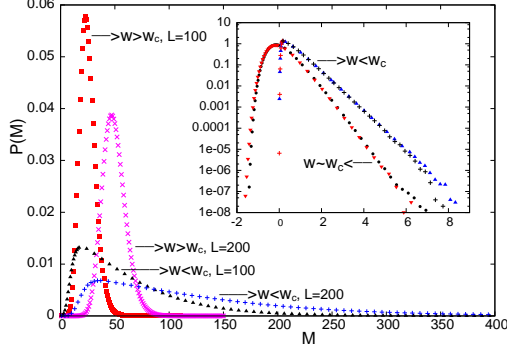


FIG. 2. $P(M)$ vs. M for $L = 100$ and $L = 200$ in the normal phase ($a = 1$, $D = 0.75$, $w = 2$) and condensate phase ($a = 1$, $D = 0.75$, $w = 0.25$). Inset: Scaling collapse of tails on plotting $LP(M)$ vs. M/L in the condensate phase and $L^{2/3}P(M)$ vs. $(M - \langle M \rangle)/L^{2/3}$ near the critical point ($a = 1$, $D = 0.75$, $w = 1.5$).

also follows $P(m_1) \sim \frac{1}{M_0} \exp\left(-\frac{m_1}{M_0}\right)$ for large m_1 [18].

- iii. The distribution of masses exiting from the left or right boundary [18] is found to follow: $P_{exit}(m) \sim \frac{1}{L^2} \left(\frac{1}{M_0} \exp\left(-\frac{m}{M_0}\right) \right)$, for large m [19].
- iv. The single site mass distribution $P(m, j, L)$ [18] follows $\frac{1}{L} f\left(\frac{j}{L}\right) \left(\frac{1}{M_0} \exp\left(-\frac{m}{M_0}\right) \right)$ at large m [19]. The factor $1/L$ arises as the aggregate can be at any one of the L sites, and $f(j/L)$ reflects that the aggregate does not visit all sites with the same probability. The rms fluctuation $\Delta m(x, L)$ of mass at a given $x = j/L$ is thus anomalously large as well: it increases as \sqrt{L} with L rather than being $\mathcal{O}(1)$, as in the normal phase.

That there is no constraint on the total number of particles per site in our model is crucial for L -dependent fluctuations to arise. Systems such as vibrated needles [20] and passive particles in fluctuating fields [21, 22] also display giant number fluctuations, but in these systems, fluctuations in a region of linear size Δl depend primarily on Δl , rather than L [10]. This is traceable to hard core interactions between particles in these models. Once this constraint is removed, macroscopic stacks can form and mass fluctuations depend on L [23].

Critical point w_c : The transition from the normal to the condensate phase takes place at a crit-

ical chipping rate w_c , which increases with injection rate a if D is held constant [24]. At criticality also, large fluctuations of the total mass are found, consistent with $\Delta M \propto L^{\theta_c}$ where $\theta_c \simeq 2/3$. The mass distribution has a tail of the form: $P(M) \sim \frac{1}{M_2} \exp\left(\frac{-(M - \langle M \rangle)}{M_2}\right)$ where $\langle M \rangle \sim L$ and $M_2 \sim L^{\theta_c}$ [inset, fig. 2]. Interestingly, we find that there is a similar L -dependent tail in the distribution of masses exiting from the left, but not the right. This is presumably because although an L -dependent aggregate forms close to the left boundary, it dissipates due to chipping on diffusing through the bulk of the system, and does not survive up to the right boundary.

Contrasting signatures of the phases also appear in dynamical properties: $M(t)$ is self-similar in time in the normal phase but exhibits breakdown of self-similarity in the condensate phase. The breakdown of self-similarity is captured in the behaviour of the structure functions $S_n(t) = \langle [M(t) - M(0)]^n \rangle$ [25] where $\langle \dots \rangle$ denotes average over histories. Self-similar signals typically show $S_n(t) \propto t^{\gamma n}$ as $t/\tau \rightarrow 0$, where γ is a constant and τ is a time scale which characterizes the lifetime of the largest structures in the system. A deviation from $S_n(t) \propto t^{\gamma n}$ reflects the breakdown of self-similarity and may occur, for example, if the signal $M(t)$ alternates between periods of quiescence (small or no activity) and bursts (sudden large changes) [12]. Such an alternation is characteristic of intermittency. The most well-studied measures of intermittency are the flatness, defined as $\kappa(t) = S_4(t)/S_2^2(t)$; and the hyperflatness $h(t) = S_6(t)/S_3^2(t)$. For intermittent signals, both $\kappa(t)$ and $h(t)$ diverge as $t/\tau \rightarrow 0$ [12]. Below we present evidence for intermittency in our model.

Normal Phase: In this phase, the structure functions are independent of L at small t and scale as $S_{2n} \sim t^{\beta_n}$ where the dependence of β_n on n is close to linear [18], indicating self-similarity of the time series $M(t)$ [fig. 3(a)]. The flatness $\kappa(t)$ and hyperflatness $h(t)$ approach a finite, L independent value as $t \rightarrow 0$ [fig. 3(c) and fig. 4 in [18]].

Condensate Phase: In the condensate phase, $M(t)$ builds up as mass is injected and drops as masses exit, with occasional large crashes [fig. 3(b)] corresponding to the exit of condensates with $\mathcal{O}(L)$ mass. The structure functions are found to scale as: $S_n \sim L^n f_n(t/L^2)$, where f_n is consistent with the form $f_n(y) \sim (-1)^n y g_n[\log(y)]$ for small y , (with g_n chosen to be a polynomial) [26], and approaches an n -dependent constant value at large y [18]. Thus,

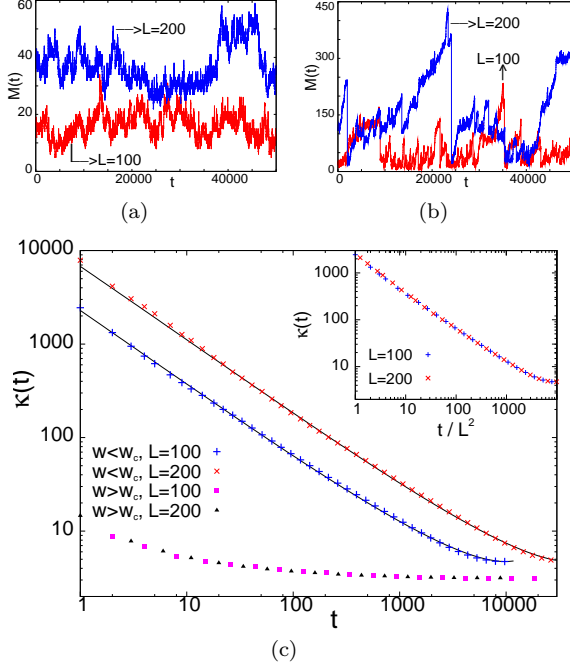


FIG. 3. (a)-(b): Realizations of $M(t)$ vs. t for different L in the (a) normal phase ($a = 1, D = 0.75, w = 3.0$) and (b) condensate phase ($a = 1, D = 0.75, w = 0.25$). Note that the y-axis in (a) and (b) has a different scale. (c) $\kappa(t)$ vs. t for $L = 100$ and $L = 200$ in the two phases. Solid lines are fits to the form described in the text for $t \ll L^2$ for $w < w_c$. Inset: Scaling collapse of $\kappa(t)$ vs. t for different L on scaling time as t/L^2 in the condensate phase.

the system shows strong intermittency: at small t , all structure functions S_n behave as $\sim t$ with the n -dependence entering only through the multiplicative $\log t$ terms. It follows that $\kappa(t)$ and $h(t)$ diverge at small times in a strongly L dependent way [fig. 3(c) and fig. 4 in [18]]. In fact, they are functions of t/L^2 and diverge as $t/L^2 \rightarrow 0$ [inset, fig. 3(c) and inset, fig. 4 in [18]]. We have also analytically calculated $S_2(t)$ in the zero chipping limit $w = 0$ [18] and find that it agrees well with numerical results.

Critical point w_c : $M(t)$ continues to show intermittency at the critical point with flatness and hyperflatness diverging as $t \rightarrow 0$ in an L dependent manner. However, there seems to be no simple scaling which collapses the curves for different L .

(B). Biased stack hopping ($D' = 0$): The steady state can be obtained exactly in the limiting cases of only chipping $D = 0$ [8] and only aggregation $w = 0$ [27]. The probability distribution of the rescaled

mass, $(M - \langle M \rangle)/\Delta M$, is Gaussian with $\Delta M \propto \sqrt{L}$, in both limits but for different reasons. In the pure chipping limit $D = 0$, this follows from the independence of masses at different sites, implied by the product measure of the mass distribution [8]; in the pure stack hopping limit $w = 0$, on the other hand, it is associated with the formation and exit of aggregates of typical size \sqrt{L} [27, 28]. This essential difference is well captured by the time series data. For $w = 0$, the total mass M shows intermittency on time scales of order \sqrt{L} , corresponding to a typical time interval of $\mathcal{O}(\sqrt{L})$ between exit events. Flatness and hyperflatness are functions of t/\sqrt{L} and diverge as power laws as $t/\sqrt{L} \rightarrow 0$. By contrast, for $D = 0$, the time series $M(t)$ is not intermittent. Thus, intermittency rather than anomalous steady state fluctuations of M , is a key signature of aggregate formation when stack hopping is driven.

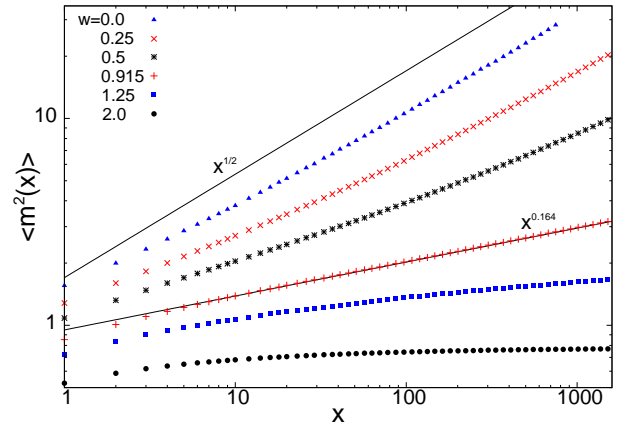


FIG. 4. $\langle m^2(x) \rangle$ vs. x for $a = 1, D = 1.5$ and different w . Note the upward (downward) bending of curves on log-log plot in aggregation (chipping) dominated phase. There is no bending at w_c .

As w is decreased, there is a phase transition from a normal phase to an aggregation-dominated phase characterized by intermittency. Unlike the unbiased case, however, the typical size of aggregates that exit the system is now expected to scale as \sqrt{L} rather than L . This is consistent with the behaviour of $\langle m^2(x) \rangle$ vs. x [fig. 4]. For large w , the plots of $\langle m^2(x) \rangle$ approach a constant value at large x , thus indicating that there are no x dependent aggregates at large x and no intermittency. For small w , the plots of $\langle m^2(x) \rangle$ vs. x bend upwards, consistent with an approach to \sqrt{x} at large x . Exit of \sqrt{L} sized aggregates leads to intermittency [18], as for $w = 0$. The transition takes place at w_c , (corresponding to

the curve with no bending on the log-log plot), at which $\langle m^2(x) \rangle$ behaves as $\sim x^{\alpha_c}$ with $\alpha_c \simeq 0.16$. $M(t)$ shows intermittency at the critical point also.

In conclusion, the principal result of this work is to establish the existence of a condensate phase in unbiased aggregation-chipping models where total mass is not conserved due to influx and outflux at the boundaries. This phase is characterized by anomalous steady state fluctuations of the total mass, and by intermittency in the dynamics, as quantified by the divergence of the flatness. It is likely that flatness would be a useful measure in other mass exchange models also. The phase transition also occurs when the movement of stacks is biased, but the intermittent, aggregation-dominated phase in this case is different.

Acknowledgements: We thank D. Dhar for useful comments on the manuscript.

-
- [1] S.N. Majumdar, Les Houches (2008) lecture notes, arXiv:0904.4097
 - [2] M. R. Evans and T. Hanney, J. Phys. A **38**, R195 (2005)
 - [3] S. N. Majumdar, S. Krishnamurthy, and M. Barma, Phys. Rev. Lett. **81**, 3691 (1998); J. Stat. Phys. **99**, 1 (2000).
 - [4] S. K. Friedlander, *Smoke, Dust and Haze* (Wiley Interscience, New York, 1977).
 - [5] V. Malhotra and S. Mayor, Nature **441**, 939 (2006)
 - [6] H. Sachdeva, M. Barma and M. Rao, Phys. Rev. E **84**, 031106 (2011)
 - [7] R. Rajesh and S. N. Majumdar, Phys. Rev. E **63**, 036114 (2001).
 - [8] E. Levine, D. Mukamel and G. M. Schütz, J. Stat. Phys. **120** 759 (2005).
 - [9] C. Connaughton, R. Rajesh, and O. Zaboronski, Phys. Rev. Lett. **94**, 194503 (2005); Physica D **222**, 97 (2006).
 - [10] S. Dey, D. Das, and R. Rajesh, Phys. Rev. Lett **108**, 238001 (2012).
 - [11] We have studied the case with reflecting boundary conditions (exit blocked from site 1) numerically and analytically in the limit $w = 0$; it also shows a similar phase transition (to be published).
 - [12] U. Frisch, *Turbulence: The Legacy of A.N. Kolmogorov*, (Cambridge Univ. Press, Cambridge, 1995).
 - [13] H. Takayasu, Phys. Rev. Lett. **63**, 2563 (1989); H. Takayasu, I. Nishikawa, and H. Tasaki, Phys. Rev. A **37**, 3110 (1988).
 - [14] Z. Cheng, S. Redner, and F. Leyvraz, Phys. Rev. Lett. **62**, 2321 (1989)
 - [15] B. Derrida, V. Hakim, and V. Pasquier, Phys. Rev. Lett. **75**, 751 (1995).
 - [16] P. L. Krapivsky and S. Redner, Phys. Rev. E **54**, 3553 (1996)
 - [17] R. Rajesh and S. Krishnamurthy, Phys. Rev. E **66**, 046132 (2002), Section VI.
 - [18] See Supplemental Material at for some analytical results in the limit $w = 0$, further numerical evidence for the differences between the two phases described in the text, and a theoretical estimate of w_c in the unbiased case.
 - [19] This holds for most $w < w_c$. For w very close to w_c , no condensate tail is visible in $P_{exit}(m)$ for right-exiting masses and in $P(m, j, L)$ for j in a small region near the right boundary.
 - [20] V. Narayan, S. Ramaswamy, and N. Menon, Science **317**, 105 (2007).
 - [21] D. Das and M. Barma, Phys. Rev. Lett. **85**, 1602 (2000); D. Das, M. Barma, and S.N.Majumdar, Phys. Rev. E **64**, 046126 (2001)
 - [22] S. Mishra and S. Ramaswamy, Phys. Rev. Lett. **97**, 090602 (2006)
 - [23] A. Nagar, M. Barma, and S. N. Majumdar, Phys. Rev. Lett. **94**, 240601 (2005); A. Nagar, S. N. Majumdar and M. Barma, Phys. Rev. E **74**, 021124 (2006).
 - [24] A rough analytical estimate for w_c is provided in the supplement. This agrees with the numerically estimated w_c to within 10%.
 - [25] This is in analogy with structure functions of the velocity field in fluid flow (see e.g. [12])
 - [26] The log terms are suggested by an analytical calculation for the $w = 0$ limit (see [18]).
 - [27] K. Jain and M. Barma, Phys. Rev. E **64**, 016107 (2001).
 - [28] S. Reuveni, I. Eliazar, and U. Yechiali, Phys. Rev. Lett. **109**, 020603 (2012).

Condensation and Intermittency in an Open Boundary Aggregation-Fragmentation Model– Supplementary Material

In this supplement, we provide the following details of analytical and numerical results for the model with unbiased stack hopping: (i) an outline of the calculation of $\langle M^n \rangle$ and $S_2(t)$ in the limit $w = 0$ of this model (ii) further numerical evidence for the differences between the condensate and normal phases, as described in the main paper (iii) a theoretical estimate of the critical chipping rate w_c . We also provide numerical evidence for intermittency in the aggregation-dominated phase of the model with biased stack hopping.

UNBIASED STACK MOVEMENT

A. Some analytical results in the limit $w = 0$:

The condensate phase extends in the range $0 \leq w < w_c$. In the zero chipping limit $w = 0$, where stack movement is the only dynamical move in the bulk, we are able to obtain some analytical results for the moments of total mass in the steady state, and the structure function $S_2(t)$. These calculations are outlined below [1].

Calculation of moments $\langle M^n \rangle$ in steady state:
To calculate moments of total mass M , we consider mass between sites $i + 1$ and j , i.e. $m_{i,j} = \sum_{k=i+1}^j m_k$ (where m_k is the mass on the k^{th} site) and the corresponding probability distribution $P_{i,j}(m)$ of this mass. In steady state, $P_{i,j}(m)$ satisfies the following equation:

$$P_{i,j+1}(m) + P_{i,j-1}(m) + P_{i-1,j}(m) + P_{i+1,j}(m) - 4P_{i,j}(m) = 0 \quad 0 < i, \quad i+1 < j, \quad j < L \quad (1a)$$

$$a[1 - \delta_{m,0}]P_{0,j}(m-1) - aP_{0,j}(m) + D[P_{0,j+1}(m) + P_{0,j-1}(m) + P_{1,j}(m) - 3P_{0,j}(m)] = 0 \quad 1 < j, \quad j < L \quad (1b)$$

$$P_{i,L-1}(m) + P_{i-1,L}(m) + P_{i+1,L}(m) - 3P_{i,L}(m) = 0 \quad 0 < i, \quad i+1 < L \quad (1c)$$

$$2\delta_{m,0} + P_{i,i+2}(m) + P_{i-1,i+1}(m) - 4P_{i,i+1}(m) = 0 \quad 0 < i, \quad i+1 = j < L \quad (1d)$$

To obtain $\langle M^n \rangle$, we now do the following:
(i) obtain recurrence relations satisfied by the generating function $Q_{i,j}(z) = \sum_{m=1}^{\infty} P_{i,j}(m)z^m$ from the

above equation (ii) differentiate $Q_{i,j}(z)$ n times to get recurrence relations for the n^{th} mass moments $\langle m_{i,j}^n \rangle$ (iii) convert the recurrence relations satisfied by $\langle m_{i,j}^n \rangle$ to a differential equation satisfied by $\langle m_{xy}^n \rangle$ by taking the continuum limit $x = i/L$, $y = j/L$ (iv) solve this differential equation (which turns out to be a Laplace equation on a triangular region) to get $\langle m_{xy}^n \rangle$ (v) substitute $x = 0$, $y = 1$ in $\langle m_{xy}^n \rangle$ to get $\langle M^n \rangle$. This gives the following expressions for $\langle M^n \rangle$, to leading order in L :

$$\begin{aligned} \langle M \rangle &= 0.5 \frac{aL}{D}, \quad \langle M^2 \rangle \sim 0.461 \left(\frac{aL}{D} \right)^2, \\ \Delta M &= \sqrt{\langle [M - \langle M \rangle]^2 \rangle} \sim 0.459 \frac{aL}{D} \\ \langle M^3 \rangle &\sim 0.615 \left(\frac{aL}{D} \right)^3, \quad \langle M^4 \rangle \sim 1.074 \left(\frac{aL}{D} \right)^4 \end{aligned} \quad (2)$$

Calculation of structure function $S_2(t)$:

$$\begin{aligned} S_2(t) &= \langle [M(t) - M(0)]^2 \rangle \\ &= 2[\langle M^2 \rangle - \langle M \rangle^2] - 2[\langle M(0)M(t) \rangle - \langle M \rangle^2] \end{aligned} \quad (3)$$

We have already calculated $\langle M^2 \rangle$ and $\langle M \rangle$. To obtain the auto-correlation function $\langle M(0)M(t) \rangle - \langle M \rangle^2$, we calculate the quantity $G_{i,j}(t) = \langle M(0)m_{i,j}(t) \rangle - \langle M \rangle \langle m_{i,j} \rangle$. This satisfies the equation:

$$\begin{aligned} \frac{\partial G_{i,j}(t)}{\partial t} &= D[\langle G_{i+1,j}(t) + G_{i-1,j}(t) + G_{i,j+1}(t) \\ &\quad + G_{i,j-1}(t) - 4G_{i,j}(t) \rangle] \end{aligned} \quad (4a)$$

$$\begin{aligned} G_{0,j}(t) &= G_{1,j}(t) \quad G_{i,L+1}(t) = G_{i,L}(t) \\ G_{i,i}(t) &= 0 \end{aligned} \quad (4b)$$

$$\begin{aligned}
G_{i,j}(0) &= \langle M m_{i,j} \rangle - \langle M \rangle \langle m_{i,j} \rangle \\
&= \frac{1}{2} [\langle m_{0,j}^2 \rangle - \langle m_{0,i}^2 \rangle + \langle m_{i,L}^2 \rangle - \langle m_{j,L}^2 \rangle] \\
&\quad - \langle M \rangle \langle m_{i,j} \rangle
\end{aligned} \tag{4c}$$

As before, we take the continuum limit $x = i/L$, $y = j/L$ in space to get a differential equation which we solve to obtain $G_{xy}(t)$ and hence $S_2(t)$. This gives the following expression for $S_2(t)$:

$$\begin{aligned}
S_2(t) &= \sum_{n=1,3,5,\dots}^{\infty} \left\{ \frac{16\eta^2}{(n\pi)^4} \left(n\pi \coth \left[\frac{n\pi}{2} \right] - 1 \right) + \frac{8\eta}{(n\pi)^2} \right\} \\
&\quad \times \left\{ 1 - \exp \left[-\frac{D\pi^2 n^2 t}{L^2} \right] \right\}
\end{aligned} \tag{5}$$

To extract the small t behaviour, we convert the above sum into an integral and take the limit $\tau = \frac{Dt}{L^2} \rightarrow 0$. In this limit, the \coth term in the above sum behaves asymptotically as $-\tau \log[\tau]$. Thus, we obtain the following small t expression for $S_2(t)$

$$S_2(t) \sim -A_0 t \log \left(A_1 \frac{Dt}{L^2} \right) \tag{6}$$

where A_0 and A_1 are some constants. Higher order structure functions can also be calculated similarly, but the calculations become very cumbersome.

B. Numerical evidence

The condensate and normal phases in the model are characterized respectively by the presence or absence of a macroscopic condensate with typical mass which is $\mathcal{O}(L)$ for a system of L sites. Signatures of this condensate appear in both the steady state and dynamical properties of the system. Below, we briefly recapitulate these properties, as presented in the main paper, and provide additional numerical evidence for them.

Steady state

In the condensate phase, the following steady state mass distributions have an exponential tail with characteristic mass $M_0 \propto L$, which we refer to as the condensate tail:

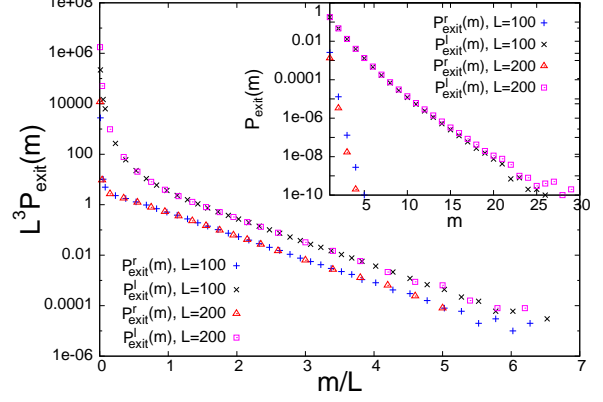


FIG. 1. Exit currents: In the condensate phase ($a = 1$, $D = 0.75$, $w = 0.25$), $P_{exit}^{l/r}(m)$ show condensate tails with good scaling collapse to $L^3 P_{exit}^{l/r}(m)$ vs. m/L for different L . Inset: In the normal phase ($a = 1$, $D = 0.75$, $w = 3.0$), exit currents do not have condensate tails.

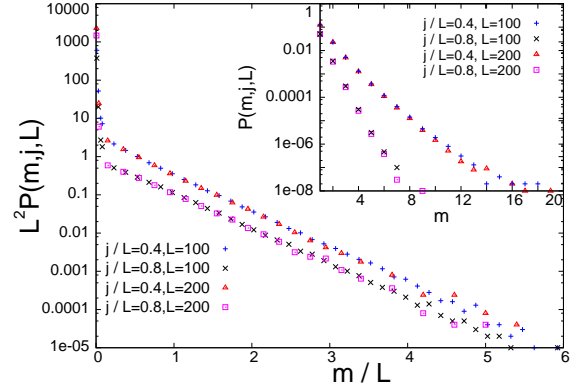


FIG. 2. Single site mass distributions: In the condensate phase ($a = 1$, $D = 0.75$, $w = 0.25$), $P(m, j, L)$ has condensate tails with the same characteristic M_0 for different j/L . There is good scaling collapse of $L^2 P(m, j, L)$ vs. m/L for a given j/L . Inset: In the normal phase ($a = 1$, $D = 0.75$, $w = 3.0$), $P(m, j, L)$ for a given j/L is independent of L to leading order and shows no condensate tail.

- i. $P(M)$: The probability distribution $P(M)$ of the total mass M in the system obeys $P(M) \sim \frac{1}{M_0} \exp \left(-\frac{M}{M_0} \right)$ for large M where $M_0 \propto L$. Evidence for this is shown in fig. 2 of main paper.
- ii. $P_{exit}(m)$: The distributions $P_{exit}^l(m)$ and $P_{exit}^r(m)$ of masses m exiting from the left and the right boundaries (i.e. sites 1 and L) respectively obey: $P_{exit}^{l/r}(m) \sim$

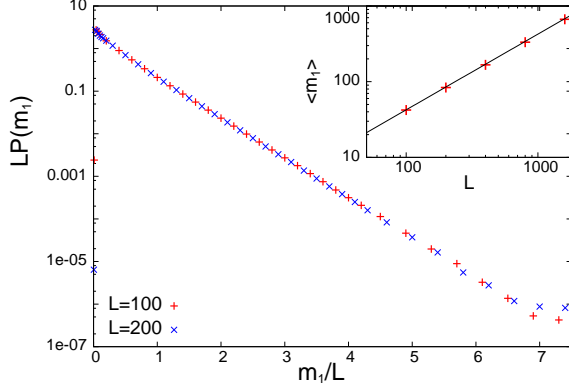


FIG. 3. Probability distribution of largest mass m_1 in the condensate phase ($a = 1$, $D = 0.75$, $w = 0.25$): $P(m_1)$ has condensate tails with good scaling collapse to $LP(m_1)$ vs. m_1/L . Inset: $\langle m_1 \rangle$ scales linearly with L .

$\frac{A_{l/r}}{L^2} \left(\frac{1}{M_0} \exp \left(-\frac{m}{M_0} \right) \right)$ at large m where the prefactor $A_{l/r}$ is different for the two distributions. Figure 1 shows the scaling collapse of the tails of the two distributions on plotting $L^3 P_{exit}^{l/r}(m)$ vs. M/L .

- iii. $P(m, j, L)$: The mass distribution at the j^{th} site of the system obeys $P(m, j, L) \sim \frac{1}{L} f \left(\frac{j}{L} \right) \left(\frac{1}{M_0} \exp \left(-\frac{m}{M_0} \right) \right)$ at large m . Figure 2 shows the scaling collapse on plotting $L^2 P(m, j/L = 0.4)$ and $L^2 P(m, j/L = 0.8)$ vs. m/L . As implied by the form of $P(m, j, L)$, for large m , the single site distributions for different j/L collapse on to different curves, which differ from each other only by the constant prefactor $f(j/L)$.
- iv. $P(m_1)$: The mass distribution of the largest mass m_1 behaves as $P(m_1) \sim \frac{1}{M_0} \exp \left(-\frac{m_1}{M_0} \right)$ for large m_1 [fig. 3]. As a result, the largest mass in the system is macroscopic (on an average), scaling as $\langle m_1 \rangle \propto L$ [inset, fig. 3]

By contrast, in the normal phase, we have:

- i. $P(M)$: The distribution for the rescaled mass variable $(M - \langle M \rangle)/\Delta M$, approaches a Gaussian at large L (see fig. 2 of main paper).
- ii. $P_{exit}(m)$: To leading order in L , $P_{exit}^l(m)$ is independent of L , while $P_{exit}^r(m) \sim (b/L)^m$ where b is a constant. (See inset in fig. 1). This behaviour of the exit currents can be

established analytically for the limiting case $D = 0$ [2].

- iii. $P(m, j, L)$: The mass distribution $P(m, j, L)$ at a given site j depends on j and L only through the rescaled position variable $x = j/L$. The inset in fig. 2 shows $P(m, j/L = 0.4)$ and $P(m, j/L = 0.8)$ vs. m for different L . Note that there is no significant dependence on L for a given j/L .
- iv. $\langle m_1 \rangle$ is sub-linear in L , such that $\langle m_1 \rangle/L \rightarrow 0$ for large L .

Dynamical properties

As discussed in the main paper, a key signature of the condensate phase is intermittency in the time series of the total mass M . This is captured by the small t behaviour of the structure functions $S_n(t)$:

Condensate phase: Numerics show that the structure functions scale with L as: $S_n \sim L^n f_n(t/L^2)$. Motivated by the small t form for $S_2(t)$ in the limit $w = 0$ (6), we use the form $f_n \sim (-1)^n y g_n[\log(y)]$ for small y , and get good fits with g_n chosen as polynomials. Figure 4(a) shows the scaling collapse of the n^{th} order structure functions for two different L to the above form for $n = 2, 4, 6$. We plot S_{2n}/\tilde{L}^2 vs t/\tilde{L}^2 (where the rescaling $\tilde{L} = L/100$ has been done to just display all three structure functions in the same plot clearly). The solid lines are fits to $t g_{2n}[\log(t/\tilde{L}^2)]$ where g_2 , g_4 and g_6 are taken to be polynomials of degrees 1, 2 and 3 respectively. The above forms of S_n imply that the flatness $\kappa(t) = S_4(t)/S_2^2(t)$ and hyperflatness $h(t) = S_6(t)/S_3^2(t)$ diverge at small t . The divergence of the flatness in the condensate phase is shown in fig. 3(c) of the main paper. Figure 5 shows the divergence of the hyperflatness, with the solid lines obtained from the fitted forms of S_6 and S_2 . The inset in fig. 5 shows the scaling collapse of $h(t)$ for different L on scaling time as t/L^2 .

Normal phase: At small times ($t \ll L^2$), the structure functions $S_n(t)$ are independent of L and behave as $S_n \sim t^{\beta_n}$ (except very close to $t = 0$), with the dependence of β_n on n being close to linear. Figure 4(b) shows S_2 , S_4 and S_6 for two different L along with solid lines t^{β_n} with $\beta_2 \sim 0.52$, $\beta_4 \sim 1.03$ and $\beta_6 \sim 1.45$. The small deviation from $\beta_n \propto n$ may be due to sub-leading correction terms. Thus, in this phase, flatness (see fig. 3(c) of main

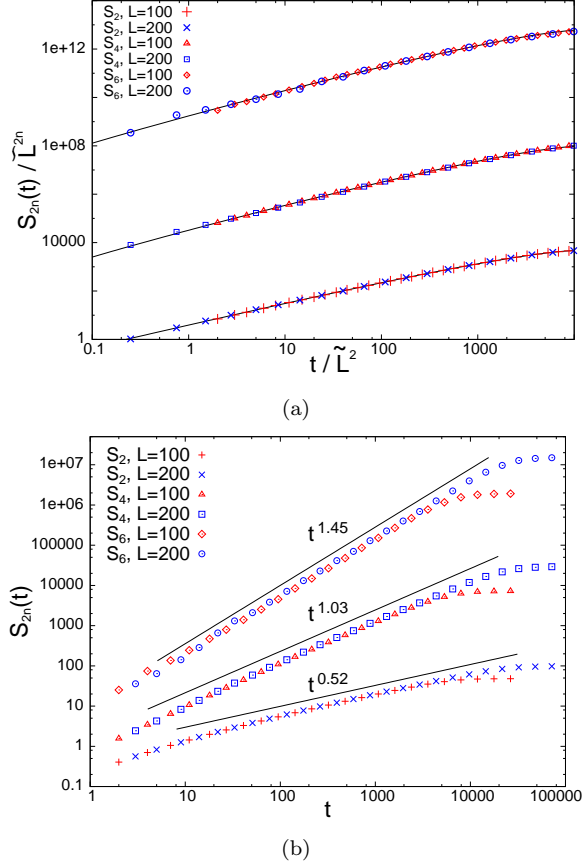


FIG. 4. Structure functions: (a) In the condensate phase ($a = 1$, $D = 0.75$, $w = 0.25$), structure functions for different L show good scaling collapse to $S_{2n}(t)/\tilde{L}^{2n}$ vs t/\tilde{L}^2 . Solid lines indicate $t g_{2n}[\log(t/\tilde{L}^2)]$ as described in text. (b) In the normal phase ($a = 1$, $D = 0.75$, $w = 3.0$), $S_{2n}(t)$ show no dependence on L and behave as $\sim t^{\beta_{2n}}$ (solid lines) for small t .

paper) and hyperflatness (fig. 5) approach finite, L independent values as $t \rightarrow 0$.

C. Estimation of critical point w_c

Let us define ρ_j and s_j respectively as the average density and occupation probability (probability that the site is non-empty) at a site j . In steady state, the balance of average mass current at each site gives the following exact expression (with D set equal to 1):

$$\rho_j + w s_j = a(1 - j/L) \quad (7)$$

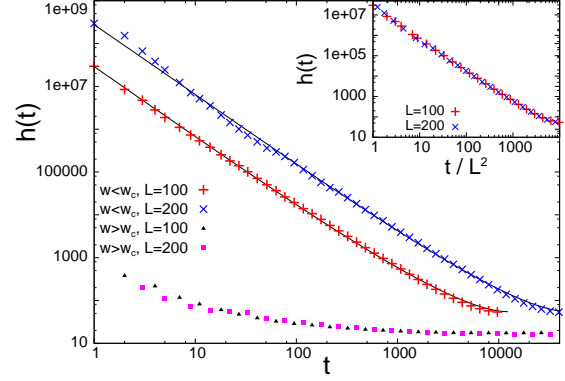


FIG. 5. $h(t)$ vs. t for $L = 100$ and $L = 200$ in the condensate ($a = 1$, $D = 0.75$, $w = 0.25$) and normal ($a = 1$, $D = 0.75$, $w = 3.0$) phases. Solid lines are fits to the form described in the text for $t \ll L^2$ for $w < w_c$. Inset: Scaling collapse of $h(t)$ vs. t for different L on scaling time as t/L^2 in the condensate phase.

We obtain a rough analytical estimate for w_c as follows: the system is in the condensate phase as long as there is at least a finite fraction of the lattice that *locally* satisfies conditions for aggregate formation. As in the closed periodic case [3], we take these conditions to be: (i) the occupation probability of a site in this region is equal to a critical occupation probability $s_c(w)$ and (ii) the mass density is greater than a critical mass density $\rho_c(w)$. While we do not have the forms of s_c and ρ_c in the open boundary case, in the limit $L \rightarrow \infty$, we approximate these by the exact conditions derived for the closed periodic case [4]:

$$s_j = s_c(w) = (\sqrt{1+w} - 1)/(\sqrt{1+w} + 1) \quad (8a)$$

$$\rho_j \geq \rho_c(w) \quad \text{where} \quad \rho_c(w) = \sqrt{1+w} - 1 \quad (8b)$$

Numerical simulations suggest that this is a reasonable approximation, at least away from the right boundary $x = L$. At w_c , a vanishingly small fraction ($j/L \rightarrow 0$) of the system satisfies conditions for aggregate formation. Thus, setting $s_j = s_c(w)$, $\rho_j = \rho_c(w)$ and $j/L \rightarrow 0$ in (7), we get:

$$w_c = (2a - 1 + \sqrt{4a + 1})/2 \quad (9)$$

This agrees with the numerically determined w_c , obtained from ΔM vs. L curves, to within 10%.

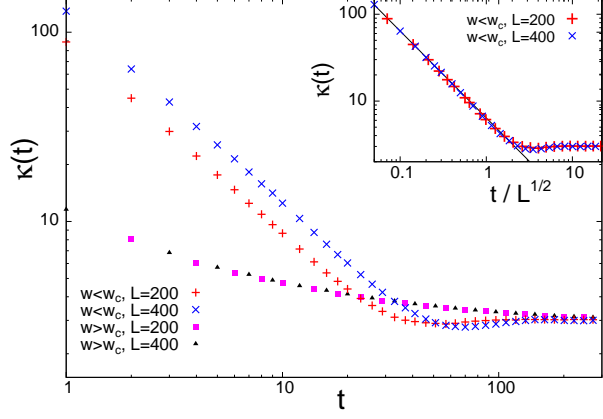


FIG. 6. Biased stack Movement: $\kappa(t)$ vs. t for $L = 200$ and $L = 400$ in the aggregation-dominated ($a = 1$, $D = 1.5$, $w = 0.125$) and normal ($a = 1$, $D = 1.5$, $w = 3.0$) phases. Inset: Scaling collapse of $\kappa(t)$ vs. t for different L on scaling time as t/\sqrt{L} in the aggregation-dominated phase. The divergence at small t roughly follows $\sim (t/\sqrt{L})^{-1}$ (solid line).

BIASED STACK MOVEMENT

When stack movement is biased, the basic signature of the aggregation-dominated phase is the in-

termittency of $M(t)$, as the steady state mass distribution $P(M)$ has the same (Gaussian) form in both phases, as explained in the main paper. Figure 6 shows the flatness $\kappa(t)$ for two different values of L in both the aggregation-dominated and normal phases. In the aggregation-dominated phase, the flatness $\kappa(t)$ diverges as $t \rightarrow 0$ in an L -dependent manner while it approaches a constant L -independent value in the normal phase. The inset in fig. 6 shows the scaling collapse of $\kappa(t)$ for different L on rescaling time as t/\sqrt{L} . Thus, intermittency occurs on time scales of order \sqrt{L} when stack hopping is biased.

-
- [1] A detailed account will be published later.
 - [2] E. Levine, D. Mukamel and G. M. Schütz, J. Stat. Phys. **120** 759 (2005).
 - [3] S. N. Majumdar, S. Krishnamurthy, and M. Barma, Phys. Rev. Lett. **81**, 3691 (1998); J. Stat. Phys. **99**, 1 (2000).
 - [4] R. Rajesh and S. N. Majumdar, Phys. Rev. E **63**, 036114 (2001).